ORIGINAL ARTICLE

AASLD
AMERICAN ASSOCIATION FOR
THE STUDY OF LIVER DISEASES

OPEN

TATA-box-binding protein promotes hepatocellular carcinoma metastasis through epithelial-mesenchymal transition

Jiayi Cao[1] | Suzhen Yang[2,3] | Tingting Luo[1] | Rui Yang[1] | Hanlong Zhu[3] | Tianming Zhao[2] | Kang Jiang[3] | Bing Xu[1] 🅾 | Yingchun Wang[4] | Fulin Chen[1]

[1]Key Laboratory of Resource Biology and Biotechnology in Western China, Ministry of Education, School of Medicine, Northwest University, Shaanxi, Xi'an, China

[2]Department of Gastroenterology, the Affiliated Drum Tower Hospital of Nanjing University Medical School, Jiangsu, Nanjing, China

[3]Department of Gastroenterology and Hepatology, Jinling Hospital, Medical School of Nanjing University, Jiangsu, Nanjing, China

[4]Department of Gastroenterology, the Affiliated Zhongshan Hospital of Dalian University, Liaoning, Dalian, China

Correspondence
Fulin Chen, Key Laboratory of Resource Biology and Biotechnology in Western China, Ministry of Education, School of Medicine, Northwest University, Shaanxi, Xi'an, 710069, China.
Email: flchen_01@126.com

Yingchun Wang, Department of Gastroenterology, Affiliated Zhongshan Hospital of Dalian University, Dalian, Liaoning 116001, China.
Email: wych_1648@126.com

Bing Xu, Key Laboratory of Resource Biology and Biotechnology in Western China, Ministry of Education, School of Medicine, Northwest University, Shaanxi, Xi'an, 710069, China.
Email: xubing@nwu.edu.cn

Abstract

Background: HCC characterizes malignant metastasis with high incidence and recurrence. Thus, it is pivotal to discover the mechanisms of HCC metastasis. TATA-box-binding protein (TBP), a general transcriptional factor (TF), couples with activators and chromatin remodelers to sustain the transcriptional activity of target genes. Here, we investigate the key role of TBP in HCC metastasis.

Methods: TBP expression was measured by PCR, western blot, and immunohistochemistry. RNA-sequencing was performed to identify downstream proteins. Functional assays of TBP and downstream targets were identified in HCC cell lines and xenograft models. Luciferase reporter and chromatin immunoprecipitation assays were used to demonstrate the mechanism mediated by TBP.

Results: HCC patients showed high expression of TBP, which correlated with poor prognosis. Upregulation of TBP increased HCC metastasis *in vivo* and *in vitro,* and muscleblind-like-3 (MBNL3) was the effective factor of TBP, positively related to TBP expression. Mechanically, TBP transactivated and enhanced MBNL3 expression to stimulate exon inclusion of lncRNA-paxillin (PXN)-alternative splicing (AS1) and, thus, activated epithelial-mesenchymal transition for HCC progression through upregulation of PXN.

Conclusions: Our data revealed that TBP upregulation is an HCC enhancer mechanism that increases PXN expression to drive epithelial-mesenchymal transition.

Abbreviations: AS, alternative splicing; ChIP, chromatin immunoprecipitation; E-Cad, E-cadherin; EMT, epithelial-mesenchymal transition; GRO-seq, Global Nuclear Run-On; H&E, hematoxylin and eosin; HK1, hexokinase 1; IHC, immunohistochemistry; MBNL3, muscleblind-like-3; N-Cad, N-cadherin; PSAT1, phosphoserine aminotransferase 1; PTPN11, protein tyrosine phosphatase, nonreceptor type 11; PXN, paxillin; RBP, RNA binding protein; RIP, RNA immunoprecipitation; RNA-Seq, RNA-sequencing; SiRNA, small interfering RNA; TBP, TATA-box-binding protein; TF, transcriptional factor; UHMK1, U2AF homology motif kinase 1.

Jiayi Cao, Suzhen Yang, Tingting Luo, and Rui Yang are the co-first authors.

Supplemental Digital Content is available for this article. Direct URL citations are provided in the HTML and PDF versions of this article on the journal's website, www.hepcommjournal.com.

INTRODUCTION

HCC remains high mortality globally for high metastatic rate.[1,2] Metastasis is the key driver of the poor prognosis in HCC patients and is, therefore, a critical target of HCC therapy.[3,4] Therefore, effective molecular and mechanisms are urgently needed to explore the new insight into HCC diagnosis and therapeutic.

Epithelial-mesenchymal transition (EMT) contributes to HCC metastasis, in which epithelial cells lose traits of adherent and polarity to transform into mesenchymal cells.[5] Correspondingly, the epithelial hallmarks became lower, while mesenchymal biomarkers improve greatly to promote tumor metastasis.[6] EMT is associated with tumor cells' identity and plasticity. Paxillin (PXN), a focal adhesion protein, adjusts cell migration to accommodate epithelial morphogenesis and embryonic development. Dramatically, PXN contains 4 isoforms generated from alternative splicing (AS), expressed in specific cell differentiation stages.[7–9] PXN-AS-L upregulates PXN level to promote NSCLC bone metastasis and HCC proliferation.[10,11] Upregulation of PXN participates in differentiation, the presence of PVT, and extrahepatic metastasis in HCC.[10] However, the mechanism of PXN in HCC metastasis is unknown.

TATA-box-binding protein (TBP) is essential for transcription initiation with multiple TBP-associated factors, located in DNA string to dynamically control gene regulation.[12–14] In yeast and human, TBP lower turnover is responsible for the higher transcriptional activity than occupancy.[15] The dynamic cycling on and off of DNA with TBP is abolished while the inhibition of the B-TFIID complex for the O-GlcNAcylation of TBP.[12] Given that transcriptional factor (TF) regulates EMT in numerous cancers, including FOX proteins,[16,17] SOX,[18] and SNAIL,[19,20] we presented whether TBP controls the pathogenesis of HCC metastatic and investigated TBP role in HCC.

In this study, we describe a novel mechanistic insight as to how TBP regulates HCC metastasis through the EMT process. Aberrant high expression of TBP correlates with a shorter overall survival rate and malignant metastasis *in vitro* and *in vivo*. TBP elevates muscleblind-like-3 (MBNL3) expression through binding to the promoter, results in exon inclusion of lncRNA-PXN-AS1, then increases PXN expression, and leads to EMT in HCC.

METHODS

HCC samples and cell lines

HCC samples and paired adjacent tissues were obtained from surgery patients of Xijing Hospital, the Air Force Military Medical University, with informed consent in compliance with the relevant ethical regulations. Tissue microarrays containing 90 cases of HCC with paired adjacent tissues and follow-up information were purchased from Outdo Biotech Co., Ltd. (Shanghai, China). Human hepatoma cell lines SK-HEP-1, PLC/PRF/5, Huh-7, SNU-398, MHCC97L, Hep3B, HCCLM6, HepG2, and HEK293FT were purchased from the American Type Culture Collection (ATCC, VA) or obtained from the State Key Laboratory of Cancer Biology (CBSKL). Cells were cultured in DMEM supplemented with 10% fetal bovine serum and penicillin-streptomycin (100 U/mL) (Gcibco, USA) in an atmosphere with 5% CO_2.

Construction of lentivirus and stable cell lines

The coding sequence (CDS) of TBP or MBNL3 was amplified through PCR reaction and cloned into the XhoI and EcoRI sites of the PLVX vector. For stable overexpression or knockdown of genes, construction vectors and shRNA were first cloned into pLKO.1 vector (Gilbert lab) using Blp1 and BstX1 sites. Then, the constructs were packaged using the lentiviral packaging system by PolyFect (QIAGEN) and Opti-MEM (Invitrogen) to transfect the constructs with packaging plasmids into HEK293FT cells. The supernatant of the virus was collected at post-transfected 48 or 72 hours and filtrated with 0.45 µM. The Hep3B and MHCC97L cells were transfected with Flag-TBP, Myc-MBNL3, and control vector and then selected with puromycin (5 µg/mL) or hygromycin B (100 µM). SNU-398 and HCCLM6 cells were transfected with shTBP, shMBNL3, and control vector and then selected with puromycin (5 µg/mL) or Geneticin (300 µg/mL). To detect PXN mRNA stability, cell lines were cultured and treated with actinomycin D (Glpbio, GC16866-5) for 0–10 hours. The reagents used in this research are listed in Supplemental Table S6, http://links.lww.com/HC9/A293.

Animal studies

Six-week-old male mice were used for xenograft experiments. HCC cells were cultured as described. Single-cell suspensions were prepared with trypsinizing and resuspending in 1X PBS on ice, and then, cells (5 × 10^6) were injected through the tail vein of mice. Tumors were allowed to grow for 8 weeks, mice were sacrificed, and lung tissues were collected for tumor morphology. Lung tissues were fixed with 4% polyformaldehyde and performed hematoxylin and eosin (H&E) staining. All the animal experiments were approved by the Animal Ethics Committee of Northwest University, which was in the compliance with the National Institutes of Health standard.

Immunohistochemistry

Tissue microarray slides (HLivH180Su16, Shanghai Outdo Biotechnology Company Ltd.) were deparaffinized and rehydrated through xylene, graded alcohols (100% ethanol, 95% ethanol, 90% ethanol, 85% ethanol, 80% ethanol, and 75% ethanol), and distilled water. Ag retrieval was performed using sodium citrate repair solution (Biosharp, BL619A) at 121 °C and continued incubation for the indicated time. Slides were incubated in 3% H_2O_2 to quench endogenous peroxidase activities at room temperature for 15 minutes and then washed 3 times in PBS. Samples were blocked with normal goad serum for 1 hour and then incubated with primary antibodies (TBP, 1:500; MBNL3, 1:1000) at 4°C overnight. Next, the secondary antibody was added for 1-hour incubation. Nuclear was stained by Diaminobenzidine (DAB) and hematoxylin followed by PBS washes. Samples were scanned by Pannoramic 250 FLASH (3DHISTECH) and performed statistics.

Western blot

Protein lysates were harvested from cells and HCC patient samples in 1X RIPA lysis buffer containing protease and phosphatase inhibitors (Millipore, USA). Protein supernatant was collected as generally described. Proteins were identified with indicated primary antibodies: TBP (Proteintech, 22006-1-AP), β-actin (Proteintech, 20536-1-AP), MBNL3 (Sigma, HPA001584), E-cadherin (E-Cad) (Proteintech, 20874-1-AP), vimentin (CST, 5741S), and PXN (Abcam, ab32115).

ChemiDoc XRS (Bio-Rad) and ImageJ were used to detect and analyze the protein expression. Antibodies and reagents are listed in Supplemental Table S5, http://links.lww.com/HC9/A293, and Supplemental Table S6, http://links.lww.com/HC9/A293.

Small interfering RNA transfection

Small interfering RNA (SiRNA) targets for TBP and PXN (GenePharma, Shanghai; Tsingke Biotechnology Co., Ltd.) were used to perform transient knockdown. HCC cells were cultured with 80%–90% density. SiRNA (100 nM) was transfected into cells using Lipo2000 (Invitrogen) indicated in the manufacturer's protocol. Knockdown efficiency was assessed by RT-qPCR or western blot as described for 48-hour post-transfection.

RNA extraction and real-time qPCR analysis

RNA was extracted with GeneJET RNA Purification Kit (Thermo Fisher, K0732), synthesized into cDNA by PrimeScript RT Master Mix (TaKaRa, RR036A), and then quantified with RT-qPCR by using QuantiNova SYBR Green PCR Kit (QIAGEN, 208054). Primer sequences used for this article are listed in Supplemental Table S2, http://links.lww.com/HC9/A293, and reagents are listed in Supplemental Table S6, http://links.lww.com/HC9/A293.

Transwell, wound healing, and colony formation assays

To assess the migration and invasion ability, HCC cells were embedded into Transwell (Corning, USA) or Matrigel Invasion Chambers. Transferred cells were harvested and stained with Crystal Violet Staining Solution (Beytomie, China) for the indicated time and obtained images. Wound healing assays were performed to detect cell migration. A cell monolayer was scratched to form a cell-free region and observed cell migration into the wound for the indicated time. In addition, colony formation was used to identify cell proliferation. Cells (1,000) were cultured for 2 weeks and stained as described. Statistical analyses were performed by ImageJ and GraphPad Prism 8.

RNA-sequencing analysis

Total RNAs were isolated using an RNeasy mini kit (Qiagen, Germany) from siControl and siTBP HCCLM6 cells. For RNA-sequencing (RNA-Seq) analysis, libraries were constructed by TruSeq RNA Sample Preparation Kit (Illumina, USA). RNA purification was performed using poly-T oligo-attached magnetic beads. Random primers were used to reverse-transcribe cDNA by DNA Polymerase I and RNase H. cDNA libraries were created from PCR enrichment, quantified using Qubit 2.0 Fluorometer (Life Technologies, USA), and validated by Agilent 2100 bioanalyzer (Agilent Technologies, USA). RNA-seq was performed on the Illumina NovaSeq. 6000 (Illumina, USA) by Sinotech Genomics Co., Ltd (Shanghai). Differential expression analysis was analyzed using R package edgeR, and gene abundance was exhibited by fragments per kilobase of exon per million reads mapped (FPKM).

Chromatin immunoprecipitation assays

HCCLM6 cells were cultured to 80%–90% confluency and washed with precold PBS. To cross-link protein to DNA, 37% formaldehyde was added into cells containing medium and incubated for 10 minutes at room temperature. Glycine was pipetted into cells to stop cross-linking within incubation for 5 minutes at room temperature. Interval washes were repeated 3 times

and cracked cells with PBS buffer (×1 protease inhibitor cocktail). Cell lysates were collected and centrifuged at 1000*g* for 10 minutes at 4 °C to discard the supernatant. Resuspend cells with 1X chromatin immunoprecipitation (ChIP) Sonication Cell Lysis Buffer, and perform sonication using optimal conditions to fragment chromatin. Next, chromatin was diluted 1:5 with 1X ChIP Buffer and divided into positive control, negative control, and immunoprecipitation group, separately including antihistone H3, normal rabbit IgG, anti-TBP, and ChIP-grade protein G magnetic beads, which were added into each IP reaction and incubated for 2 hours at 4 °C with rotation. Follow-up to salt wash with low grade to high grade; Antibody/protein G beads were obtained and eluted chromatin supernatant with 1X ChIP Elution Buffer. Precipitated chromatin was de-cross-linked and purified using Spin Columns (Simple-ChIP Plus Sonication ChIP Kit, CST, 56383S). DNA samples were analyzed by PCR using specific promoter primers of MBNL3. ChIP primers are listed in Supplemental Table S3, http://links.lww.com/HC9/A293.

Luciferase reporter assay

Luciferase reporter plasmids were constructed using pRL-TK, pRL-SV40, or pRL-CMV (Promega, Madison, WI) by LipofectamineTM 2000 (Invitrogen, Carlsbad, CA) according to the manufacturer's instruction. 293T cells were cultured and transfected with established plasmids. Luciferase activity was measured using the Dual-Luciferase Reporter Assay System (Promega) at 48-hour post-transfection. Data were calculated using the normalized method between a firefly and renilla luciferase activity and then analyzed by GraphPad Prism 8.

RT-PCR and splicing assays

Total RNAs were isolated and reverse-transcribed into cDNA as described. Interest targets were amplified by PCR with a 0.5-µg cDNA template using T3 Super PCR Mix (Tsingke Biotechnology Co., Ltd.). PCR products were separated with 2% agarose gel and pictured by SYSTEM GelDoc XR+ IMAGE LAB (Bio-Rad). Quantification was calculated by using ImageJ. Primers of AS are listed in Supplemental Table S4, http://links.lww.com/HC9/A293.

RNA immunoprecipitation assays

Cells were harvested and washed with precold PBS and resuspended in a complete RNA immunoprecipitation

(RIP) lysis buffer (Protease Inhibitor Cocktail, RNase Inhibitor, Millipore). Lysates were incubated on ice for 5 minutes. Magnetic beads were washed with RIP Wash Buffer and incubated rotating with antibody for 30 minutes at room temperature. Cell supernatants were collected, mixed with RIP Immunoprecipitation Buffer (0.5 M EDTA, RNase Inhibitor), and added beads-antibody complex incubating rotation at 4 °C overnight. RIP complexes were washed several times with wash buffer and digested protein heating to 55 °C and incubated with proteinase K buffer (RIP Wash Buffer, 10% SDS, Proteinase K). Phases were separated through centrifugation, which is mixed with organic reagents (phenol: chloroform: isoamyl). Then, aqueous phases were extracted continually with chloroform and then precipitated with Salt Solution I, Salt Solution II, and Precipitate Enhancer. Pellet was washed with 80% ethanol and suspended in RNase-free water. RNA samples were reverse-transcribed and quantified cDNA templates using QuantiNova SYBR Green PCR Kit (QIAGEN) amplified with RIP primers. PCR products were detected by 2% agarose gel simultaneously with verification of qPCR results.

Immunofluorescence

Stable cell lines were cultured into appropriate density. Paraformaldehyde was used to fix cells and removed nonspecific antigens by 5% BSA (Aladdin). Primary antibodies were used as indicated: E-Cad (1:100, Proteintech, 20874-1-AP), Vimentin (1:150, CST, 5741S), and PXN (1:200, Abcam, ab32115) at 4 °C overnight. On the next day, cells were washed with PBS 3 times and then incubated with secondary antibodies of CoraLite 488-conjugated Affinipure Goat Anti-Rabbit IgG (1:200, Proteintech, SA00013-2) and CL594-conjugated mouse anti-rabbit IgG (1:200, Proteintech, CL594-66467) for 1 hour. Nuclear was stained with DAPI (Yeasen, 40728ES10) for 10 minutes at room temperature. Slides were coated with ProLong Gold and Diamond Antifade Mountants (Invitrogen, P10144). Images were scanned by FLUOVIEW FV3000 (Olympus). The reagents are listed in Supplemental Table S6, http://links.lww.com/HC9/A293.

Quantification and statistical analysis

All experiments were performed in biological and technological replicates. Statistical analyses were performed using GraphPad Prism 8 for Student *t* test (2-sided) and Pearson correlation analysis. Quantification was calculated using

ImageJ software. Significance was expressed as $p < 0.05$.

RESULTS

Upregulation of TBP is significantly associated with poor prognosis in HCC patients

To identify the clinical role of TBP in HCC patients, we first assessed TBP expression by immunohistochemically staining. The results exhibited that TBP was highly expressed in HCC tissues (Figure 1A, $p < 0.001$). Most notably, HCC patients with higher TBP levels showed relatively shorter overall survival time compared with those with lower TBP expression (Figure 1B. $p < 0.01$). Upregulation of TBP mRNA was validated in 36 pairs of HCC and corresponding adjacent nontumorous tissues from surgery patients (Figure 1C, 2.85 ± 2.51 versus 0.52 ± 0.36, $p < 0.001$). Consistently, TBP protein expression was strongly increased in HCC patients confirmed by western blotting assays (Figure 1D). The expression of TBP mRNA and protein was higher in HCC cell lines than in normal liver tissues (Figure 1E, F).

All those data suggested that TBP expression is closely related to HCC carcinogenesis and the prognosis of HCC patients.
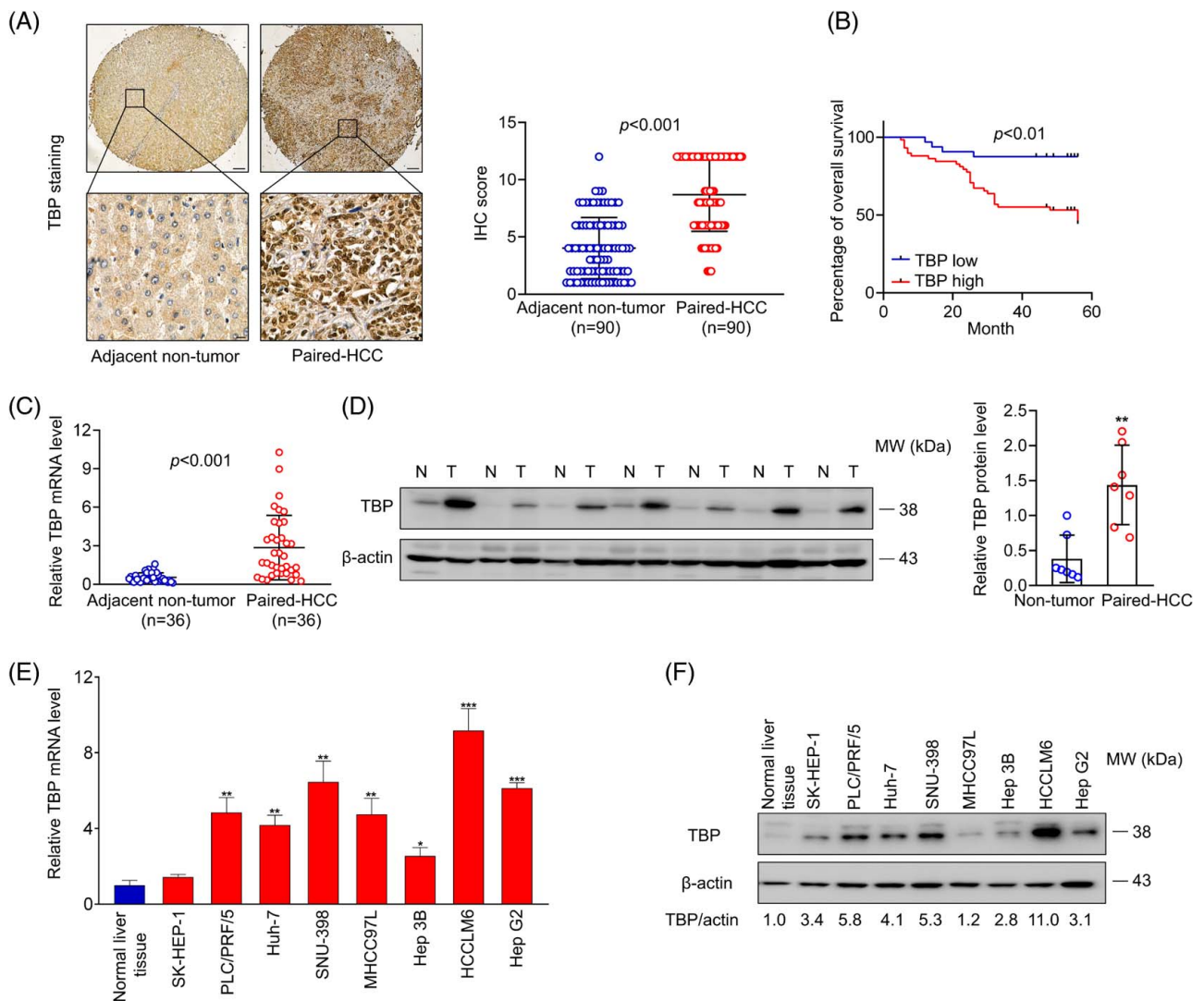

FIGURE 1 Upregulation of TBP is remarkably associated with poor prognosis in HCC patients. (A) IHC staining TBP in adjacent nontumor tissues and HCC tissues (n = 90). Scale bars: 100 μm (upper) and 10 μm (lower). (B) Kaplan–Meier analysis of the relationship between TBP level and overall survival time of HCC patients. (C) Real-time RT-PCR analysis of TBP mRNA level in adjacent nontumor tissues and HCC tissues (n = 36). (D) Western blot analysis of TBP protein expression in adjacent nontumor tissues and HCC tissues. (E) Real-time RT-PCR analysis of TBP mRNA level in normal liver tissues and HCC cell lines. (F) Western blot analysis of TBP protein expression in HCC normal liver tissues and HCC cell lines. For (A–E), data are mean $\pm$ SD of n = 3 independent experiments, $*p < 0.05$, $**p < 0.01$, and $***p < 0.001$ by Student t test. Abbreviations: IHC, immunohistochemistry; TBP, TATA-box-binding protein.

TBP is required for HCC progression *in vitro* and *in vivo*

To investigate the function of TBP in HCC progression, we performed gain and loss functional detection *in vitro* and *in vivo*. First, we constructed and verified stable models of TBP overexpression in Hep 3B and MHCC97L cells, and established shRNA-TBP-

knockdown clones in HCCLM6 and SNU-398 cells (Figure 2A). Overexpression of TBP drastically facilitated HCC cells' invasion and migration capacities. Conversely, endogenous knockdown of TBP distinctly suppressed the invasion and migration rate of HCCLM6 and SNU-398 cells (Figure 2B, C). Further evaluation of wound healing assays proved the markedly high rate of migration when upregulation of TBP, while
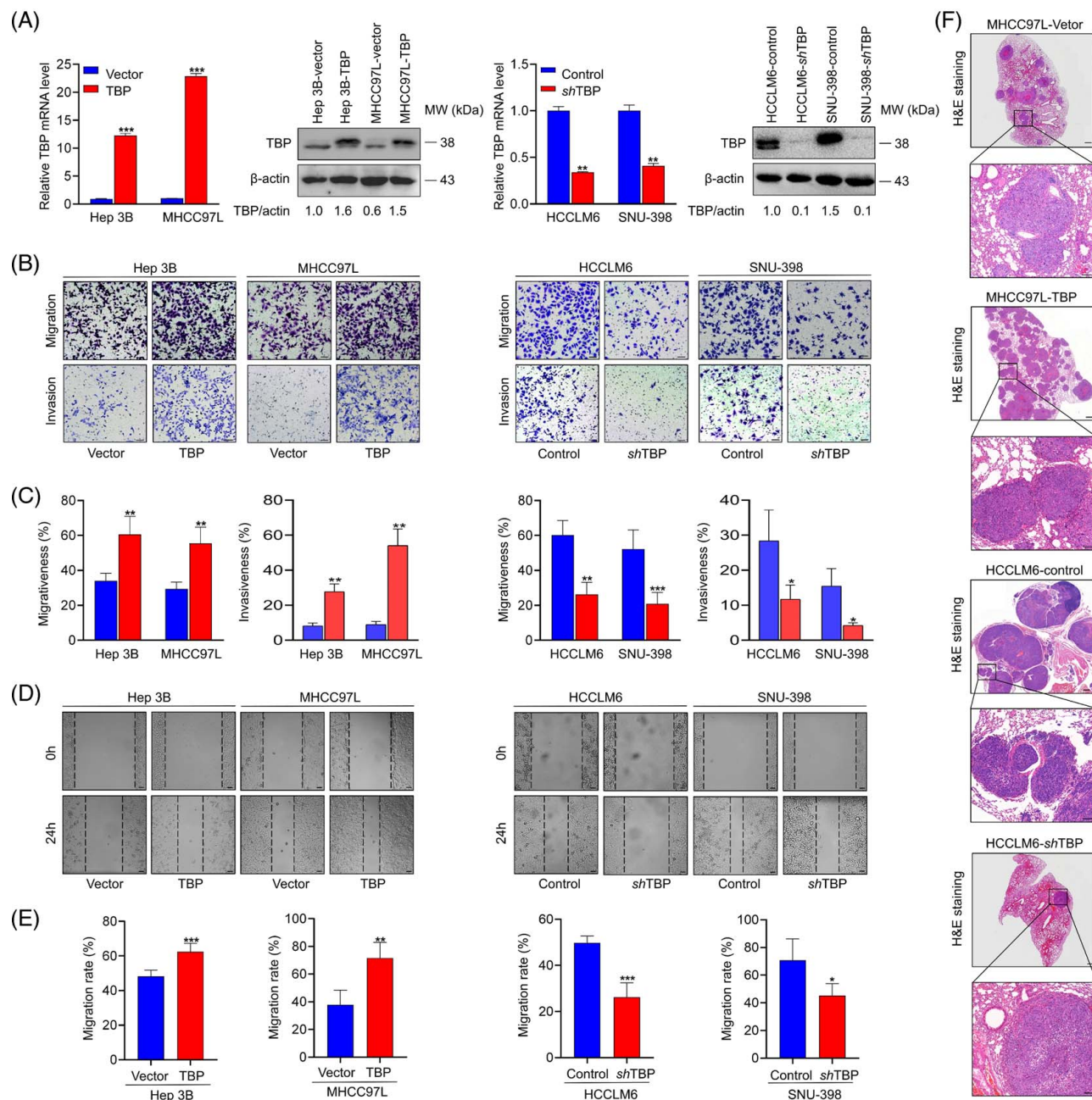

FIGURE 2   TBP is required for HCC progression *in vitro* and *in vivo*. (A) Real-time RT-PCR and western blot analysis of TBP expression in the indicated cell lines after lentiviral transfection. (B and C) Transwell assays indicated that the TBP overexpression promoted the migration and invasion ability of Hep 3B and MHCC97L cells, whereas TBP knockdown abrogated the migration and invasion ability of HCCLM6 and SNU-398 cells. Scale bars: 20 μm. (D and E) Wound healing assays indicated that the TBP overexpression promoted the migration rate of Hep 3B and MHCC97L cells, whereas TBP knockdown abrogated the migration rate of HCCLM6 and SNU-398 cells. Scale bars: 20 μm. (F) Representative H&E-stained sections of lung samples from different groups. Scale bars; 500 μm (upper) and 100 μm (lower). For (A), (C), and (E), data are mean ± SD *$p < 0.05$, **$p < 0.01$, and ***$p < 0.001$ by Student *t* test. Abbreviations: H&E, hematoxylin and eosin; TBP, TATA-box-binding protein.

downregulation of TBP slowed down the rate of migration in HCC cells (Figure 2D, E). To better assess the prometastatic role of TBP in HCC, we established the *in vivo* study by injecting MHCC97L-TBP, HCCLM6-shTBP, and their corresponding control cells in nude mice through the tail vein. Histological analysis reveals that high TBP expression induced more metastasis nodules, whereas low expression of TBP reduced the number of metastasis nodules in lung tissue (Figure 2F). Besides, colony formation assays confirmed that MHCC97L and Hep 3B cells' stably overexpressing TBP promotes cell proliferation, while that was reduced in TBP stably silenced HCCLM6 and SNU-398 cells (Supplemental Figure S1A, B, http://links.lww.com/HC9/A390). Taken together, these data indicated that TBP promoted HCC progression.

TBP promotes EMT induction in HCC cells

Metastasis matters most to the high recurrence rate of HCC patients.[21]

The EMT significantly attributes to the early stage of tumor metastasis; especially, the mesenchymal phenotype becomes more pronounced.[4] More epithelial morphology was presented when TBP was downregulated, whereas a more fibroblast-like shape was found when TBP was overexpression (Figure 3A). Further specifically, expression of mesenchymal marker N-cadherin (N-Cad) was remarkably increased, as well as vimentin level, when TBP was overexpressed but suppressed E-Cad to induce the EMT process (Figure 3B). The association between TBP and EMT was validated by immunofluorescence staining, indicating that enhanced expression of TBP promotes N-Cad and vimentin expression, with restrained E-Cad expression (Figure 3C, right). On the contrary, depletion of TBP resulted in the downregulation of Vimentin and N-Cad but upregulated E-Cad expression (Figure 3C, left), which is consistent with the results of mRNA expression (Figure 3D). These data concluded that TBP caused HCC development through the EMT process.

MBNL3 is required in TBP-driven HCC metastasis

To explore in-depth mechanisms by which TBP regulates EMT in HCC metastasis, we performed RNA-sequencing (RNA-seq) analysis to identify downstream effectors. Next, the candidate target molecules were quantified consisting of hexokinase 1 (HK1), phosphoserine aminotransferase 1 (PSAT1), protein tyrosine phosphatase, nonreceptor type 11 (PTPN11), U2AF homology motif kinase 1 (UHMK1),

and MBNL3 (Figure 4A and Supplemental Figure S3, http://links.lww.com/HC9/A295). Both PSAT1 and MBNL3 levels were regulated by ectopic expression or endogenous knockdown of TBP. PSAT1, a metabolic enzyme, plays a metabolic and nonmetabolic function in carcinogenesis, involved in serine biosynthesis and, moreover, elevating in lung adenocarcinoma for EGFR inhibitor resistance and tumor metastasis.[22] Most strikingly, MBNL3 is upregulated in fetal livers, depleted in adult livers, and restored high expression in HCC patients. These demonstrated that MBNL3 is critical for liver evolution and especially for HCC tissues. Hence, we focused on MBNL3 and further evaluated its role in HCC. We then evaluated MBNL3 mRNA expression in HCC samples and found that the expression of MBNL3 is significantly higher in HCC tissues compared with nontumorous tissues (2.76 ± 2.31 vs. 0.66 ± 0.57, $p < 0.001$, Figure 4B), as well as upregulation of MBNL3 in HCC patients (Figure 4C and Supplemental Figure S2A, http://links.lww.com/HC9/A294). Moreover, MBNL3 expression was positively correlated with TBP expression both in mRNA and protein levels of HCC samples (Figure 4D and Supplemental Table S1, http://links.lww.com/HC9/A293). Increased MBNL3 levels in HCC patients predict unsatisfied overall survival (Supplemental Figure S2B, http://links.lww.com/HC9/A294). Transwell assay demonstrated that upregulation of MBNL3 promoted invasion and migration capacities, while knockdown of MBNL3 repressed these abilities of HCC cells *in vitro* (Figure 4E). Interestingly, silenced MBNL3 in TBP overexpression cells dramatically alleviated the invasion and migration rate caused by TBP upregulation *in vitro* and suppressed tumor metastasis *in vivo* (Figure 4F), and overexpressed MBNL3 in knockdown of TBP cells rescued both metastases of HCC cells (Supplemental Figure S4, http://links.lww.com/HC9/A391). Collectively, all these data demonstrated that MBNL3 is regulated by TBP in HCC progression.

TBP/MBNL3/lncRNA-PXN-AS1/PXN signaling facilitates the metastasis of HCC cells

TBP has been discovered to involve in the formation of a preinitiation complex within binding to core promoter DNA.[23] To elucidate the molecular mechanism underpinning MBNL3-regulated by TBP, we next sought to perform luciferase assays. Surprisingly, the relative luciferase activity was significantly increased in cells cotransfected with the MBNL3 promoter and pcDNA3.1-TBP than the control group, indicating that TBP activated MBNL3 in the transcriptional level (Figure 5A). Putative analyses of binding sites were
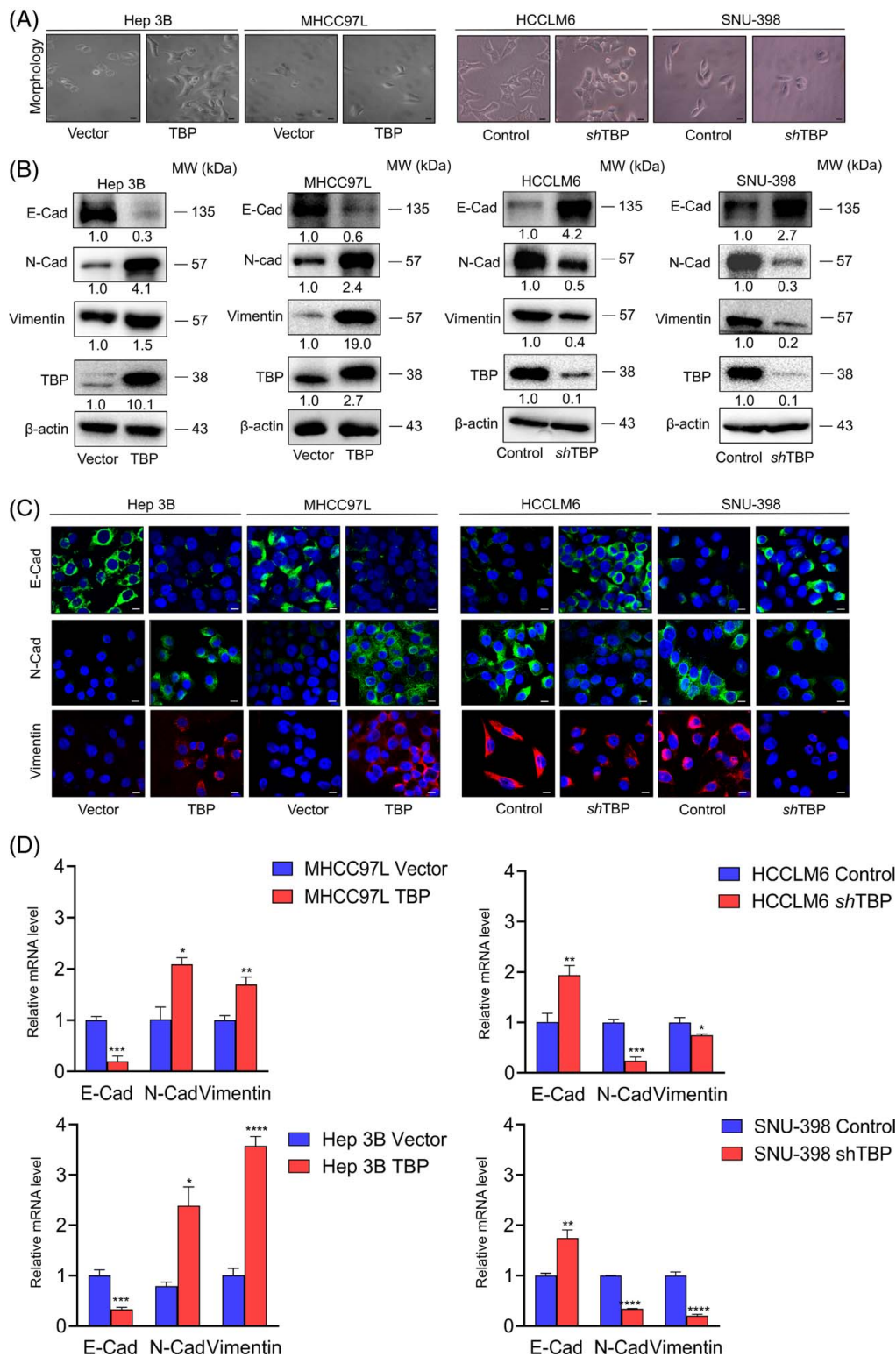
FIGURE 3 TBP promotes epithelial-mesenchymal transition (EMT) induction in HCC cells. (A) Representative images of morphology changes of indicated cell lines. Scale bars: 20 μm. (B) Western blot analysis of EMT-related markers of indicated cell lines. (C) Representative immunofluorescence staining of EMT-related markers of indicated cell lines. Blue: DAPI. Red: Vimentin. Green: E-Cad and N-Cad. Scale bars: 10 μm. (D) Real-time RT-PCR analysis of EMT markers' expression in the indicated cell lines. Data are mean ± SD of n = 3 independent experiments, *$p < 0.05$, **$p < 0.01$, ***$p < 0.001$, and ****$p < 0.0001$ by Student t test. Abbreviations: E-Cad, E-cadherin; N-Cad, N-cadherin; TBP, TATA-box-binding protein.
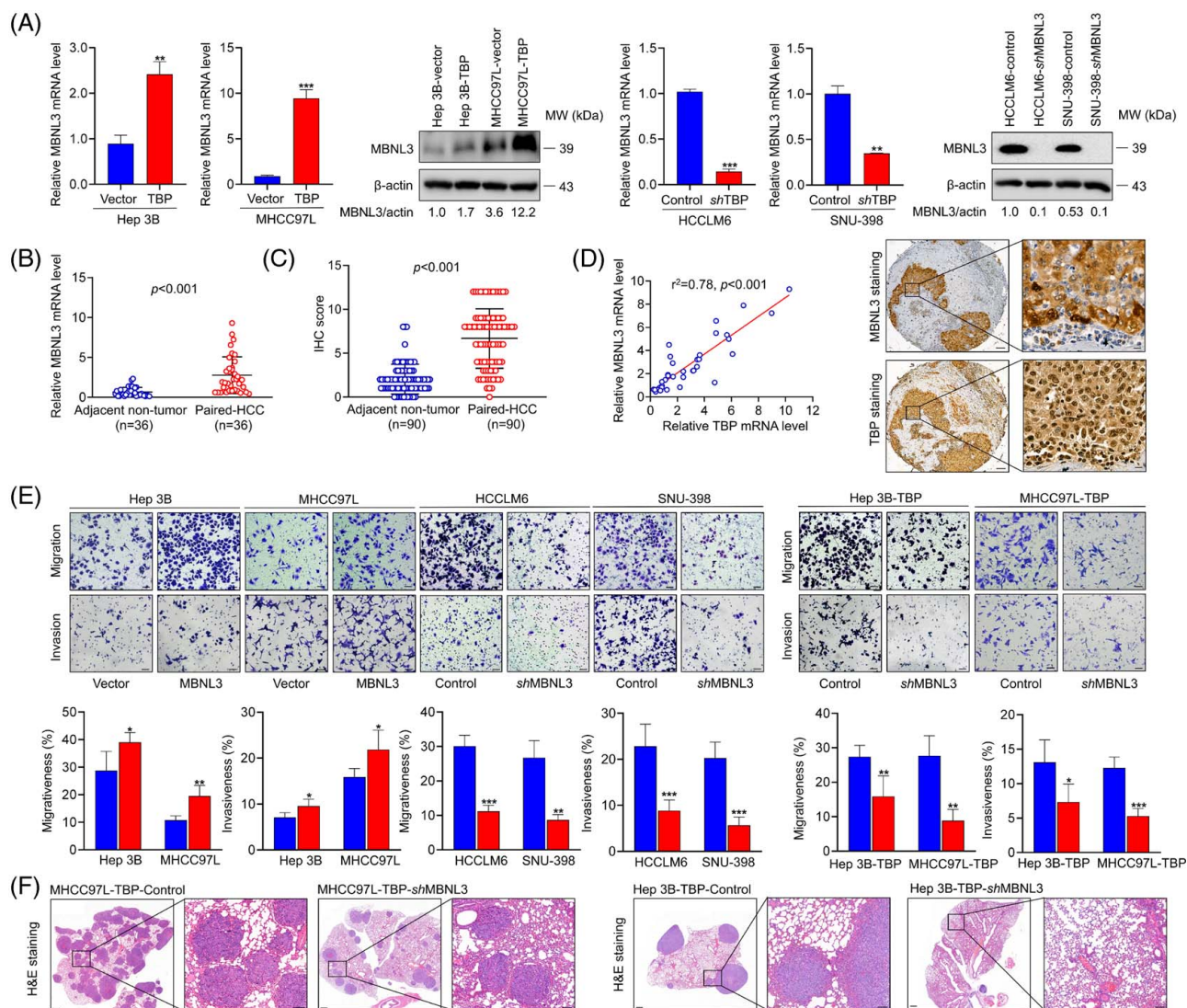
FIGURE 4 MBNL3 is regulated by TBP in HCC metastasis. (A) Real-time RT-PCR and western blot analysis of MBNL3 expression in the indicated cell lines after lentiviral transfection. (B) Real-time RT-PCR analysis of MBNL3 mRNA level in adjacent nontumor tissues and HCC tissues (n = 36). (C) Correlations between MBNL3 and TBP mRNA expression. (D) IHC score of MBNL3 in adjacent nontumor tissues and HCC tissues (n = 90), and representative IHC images of MBNL3 and TBP expressions. Scale bars: 100 μm (left) and 10 μm (right). (E) Transwell assays (top) indicated that the MBNL3 overexpression promoted the migration and invasion ability of Hep 3B and MHCC97L cells, whereas MBNL3 knockdown abrogated the migration and invasion ability of HCCLM6 and SNU-398 cells; in addition, knockdown of MBNL3 in TBP overexpression cells dramatically alleviated the invasion and migration rate caused by TBP upregulation (bottom). Scale bars: 20 μm. (F) Representative H&E-stained sections of lung samples from different groups. Scale bars: 500 μm (left) and 100 μm (right). For (A–E), data are mean $\pm$ SD of n = 3 independent experiments, $*p < 0.05$, $**p < 0.01$, and $***p < 0.001$ by Student t test. Abbreviations: MBNL3, muscleblind-like-3; TBP, TATA-box-binding protein.

implemented through the JASPAR database and next verified TBP-binding sites through mutation assays of luciferase activity (Figure 5B, C). Together with the result of the ChIP assay, we indicated that TBP transcriptional activated MBNL3 (Figure 5D). MBNL3, as a splicing factor, has been reported to promote HCC through AS of lncRNA-PXN-AS1.[24] To investigate whether TBP could affect lncRNA-PXN-AS1 exon 4 inclusion through transcriptional activates MBNL3, we accomplished relevant experiments for validation. As expected, overexpression of TBP stimulated exon 4 inclusion, while depletion of TBP repressed exon 4 inclusion, and

the increased exon 4 inclusion caused by TBP upregulation can be repressed by MBNL3 knockdown (Figure 5E).

A previous study has suggested that MBNL3 induces lncRNA-PXN-AS1 exon 4 inclusion to upregulate PXN level, contributing to HCC progression.[24] Combining these results, we hypothesize that transactivated MBNL3 by TBP might be responsible for the upregulation of PXN to accelerate HCC progression. Indeed knockdown of MBNL3 significantly inhibited PXN expression in ectopic expression of TBP (Figure 5F, G). These data demonstrated that TBP promotes HCC metastasis
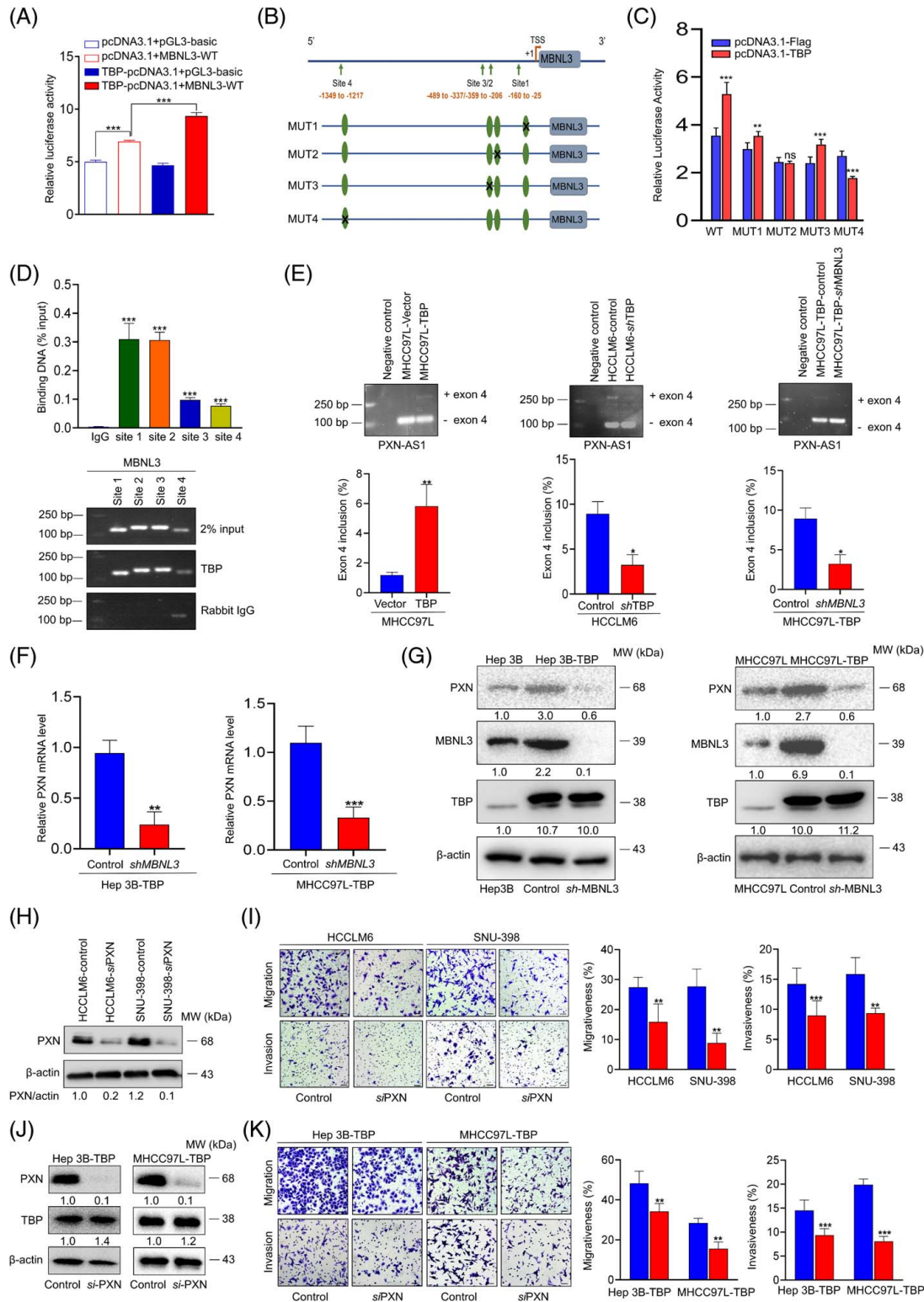
FIGURE 5 TBP transcriptional activates MBNL3 expression to facilitate PXN expression through lncRNA-PXN-AS1 exon 4 inclusion. (A–C) Luciferase reporter assay was performed to detect promoter activities of MBNL3 transcriptionally regulated by TBP. Then, mutated-MBNL3 promoter constructs were cotransfected with pcDNA3.1-TBP, and the relative luciferase activity was determined. Relative luciferase activity represented the ratio of firefly luciferase activity to renilla luciferase activity. (D) Chromatin immunoprecipitation (ChIP) assay was performed to confirm that TBP transcriptional activates MBNL3 expression. (E) Inclusions of exon 4 of PXN-AS1 were examined in indicated cells. (F and G) Real-time RT-PCR and western blot analysis of PXN expression in the indicated cell lines after lentiviral transfection. (H) Western blot analysis of PXN expression in the indicated cell lines. (I) Transwell assays indicated that the PXN knockdown abrogated the migration and invasion ability of HCCLM6 and SNU-398 cells. Scale bars: 20 μm. (J) Western blot analysis of PXN expression in the indicated cell lines. (K) Transwell assays indicated that the PXN knockdown alleviated the invasion and migration rate caused by TBP upregulation. Scale bars: 20 μm. For (A–E), data are mean ± SD of n = 3 independent experiments, *$p < 0.05$, **$p < 0.01$, ***$p < 0.001$, ns, and $p > 0.05$ by Student t test. Abbreviations: MBNL3, muscleblind-like-3; PXN, paxillin; TBP, TATA-box-binding protein.

depending on transcriptional activation of MBNL3, resulting in lncRNA-PXN-AS1 exon 4 inclusion, and eventually upregulates PXN.

PXN is a focal adhesion protein, which affects cytoskeletal rearrangements, as well as tissue remodeling and cell motility.[7] The augmented levels of PXN promote cancer metastasis and invasion.[10,25]

Therefore, we confirmed the PXN function by interfering with its expression in HCCLM6 and SNU-398 cells (Figure 5H). Knockdown of PXN significantly suppressed cell invasion and migration (Figure 5I). Surprisingly, silenced PXN in Hep 3B-TBP and MHCC97L-TBP cells dramatically mitigated TBP-induced invasion and migration (Figure 5J, K). These data demonstrated that TBP promotes HCC cell invasion and migration by regulating PXN expression.

DISCUSSION

HCC patients have the extremely lowest survival rate for the malignant metastasis of liver cancer. Moreover, metastasis is also the main course of HCC recurrence rate post-treatment.[26] Given the complexity and diversity of the etiology of HCC metastasis, molecular mechanism research needs to be eagerly carried out. Our study presented a novel perspective of TBP involved in HCC progression through the regulation of metastasis. Tissue array assays and HCC samples' expression of TBP demonstrate that the TBP level is clinically significant. High TBP expression connects with the poor prognosis of HCC patients. Further RNA sequencing identified MBNL3 as a critical TBP target in HCC. Following luciferase activity and ChIP results uncovered TBP binds to the MBNL3 promoter and activate MBNL3, which stimulated exon inclusion of lncRNA-PXN-AS1, resulting in the upregulation of PXN for inducing the EMT process. These data strongly suggested that TBP/MBNL3/lncRNA-PXN-AS1/PXN axis facilitates HCC metastasis through the EMT process.

TBP recruits associated factors to assemble the preinitiation complex, driving transcription initiation in mammalian cells.[27,28] The precision and complexity of eukaryotic transcription initiation systems were generated through the asymmetric structure of TBP. Based on the leading role in transcription initiation, TBP is expressed widely with low tissue specificity except for testis.[29,30] Consistently, data from HCC patients and HCC cell lines verified the upregulation of TBP, particularly in HCCLM6 cells of high metastasis. Upregulation of TBP significantly facilitated the invasion and migration of HCC cells and lung metastasis *in vivo*, whereas knockdown of TBP extremely attenuated the above process. EMT plays a critical role in HCC metastasis.[5] Mesenchymal markers (N-Cad and vimentin) level increased in HCC cells of upregulation

TBP, coupled with epithelial marker E-Cad expression decreased. These results highlighted the dramatic role of TBP associated with HCC metastasis through EMT.

Downstream targets of TBP were screened and identified through RNA-sequencing, including MBNL3, HK1, PSAT1, PTPN11, and UHMK1. As an AS regulator, MBNL3 controls gene expression.[31] Previous studies demonstrated that MBNL3 affects radio sensitivity and paclitaxel resistance in carcinogenesis.[32,33] MBNL3 is overexpressed in HCC, although likewise PSAT1. However, MBNL3 is an HCC-specific oncofetal protein for the unique therapeutic target of HCC, which overexpressed in fetal liver tissues, silenced in adult liver and reproduced in HCC tissues.[24] TBP positively correlated with MBNL3 expression and transactivated MBNL3 expression by directly binding to its promoter. Inhibition of MBNL3 suppressed TBP-induced HCC metastasis, while exogenous increased MBNL3 level enhanced the low metastasis caused by TBP depletion. Given that transcriptional factor dynamically binds to target sites, meanwhile, MBNL3 was expressed with spatial–temporal specificity. Beyond the binding sites of MBNL3 and TBP, whether TBP binds to MBNL3 involved cycles of association and disassociation is yet to be investigated.

MBNL3 promotes HCC through AS of lncRNA-PXN to regulate PXN expression for HCC proliferation.[24] PXN is a cytoplasmic protein that regulated focal adhesion and cell motility, promoting cancer metastasis through EMT acceleration.[7,25] Oncogenic isoform of PXN-AS1 regulated HCC metastasis through DDX17-mediated AS events.[34] Interestingly, our study determined that TBP transcriptional actives MBNL3 and subsequently alerts lncRNA-PXN-AS1 exon 4 inclusion to modulate PXN level. More importantly, increased exon 4 inclusion in TBP upregulation was repressed by knockdown MBNL3. In addition, colony formation within upregulation or downregulation of TBP identified that the proliferation of HCC cells correlates with TBP level, inhibition of MBNL3 suppressed HCC cells proliferation in TBP-overexpressed, and upregulation of MBNL3 enhanced the minority clone of HCC cells in TBP depletion. Knockdown PXN decreased, and interference of PXN suppressed the majority clone of HCC cells in TBP upregulation (Supplemental Figure S1, http://links.lww.com/HC9/A390).

RNA binding protein (RBP) mediates AS to directly control gene expression, such as RBM25, XRCC5, and U2AF1 through Global Nuclear Run-On (GRO-seq). Integrated with the ChIP-seq database of RBPs and TFs, researchers propose that RBP regulates gene expression as TF or TF-associated factors like RBM25 coregulate gene expression with YY1.[35] One-third of AS regulators are TF, regulating AS with dual effects to control gene expression; one is to increase splicing factors expression, besides binds to pre-mRNA.[36] More important, endogenous knockdown of PXN

dramatically suppressed the TBP-induced invasion and migration of HCC cells *in vitro*. Thus, we questioned whether TBP could directly regulate PXN expression by controlling AS process. Interestingly, TBP, expressed in nuclear, might be a potential RBP binding to PXN mRNA, influencing its stability and, thus, adjusted PXN expression Supplemental Figure S5, http://links.lww.com/HC9/A296. However, the specific role and mechanism of TBP in AS of HCC metastasis are still unclear, which ought to interpret with further exploration.

In summary, our study demonstrates that high expression of TBP is a poor prognosis in HCC. TBP promotes HCC metastasis through the transactivation of MBNL3 to upregulate PXN for EMT induction. Taken together, our study proposes a mechanistic link between TBP and HCC metastasis to comprehend TBP's potential role as a diagnostic marker in HCC.

CONFLICTS OF INTEREST

The authors have no conflicts to report.

ORCID

Bing Xu https://orcid.org/0000–0001–7720–6363

REFERENCES

1. Bray F, Ferlay J, Soerjomataram I, Siegel RL, Torre LA, Jemal A. Global cancer statistics 2018: GLOBOCAN estimates of incidence and mortality worldwide for 36 cancers in 185 countries. CA Cancer J Clin. 2018;68:394–424.
2. Llovet JM, Castet F, Heikenwalder M, Maini MK, Mazzaferro V, Pinato DJ, et al. Immunotherapies for hepatocellular carcinoma. Nat Rev Clin Oncol. 2022;19:151–72.
3. Lambert AW, Pattabiraman DR, Weinberg RA. Emerging biological principles of metastasis. Cell. 2017;168:670–91.
4. Giannelli G, Koudelkova P, Dituri F, Mikulits W. Role of epithelial to mesenchymal transition in hepatocellular carcinoma. J Hepatol. 2016;65:798–808.
5. van Zijl F, Zulehner G, Petz M, Schneller D, Kornauth C, Hau M, et al. Epithelial-mesenchymal transition in hepatocellular carcinoma. Future Oncol. 2009;5:1169–79.
6. Zeisberg M, Neilson EG. Biomarkers for epithelial-mesenchymal transitions. J Clin Invest. 2009;119:1429–37.
7. López-Colomé AM, Lee-Rivera I, Benavides-Hidalgo R, López E. Paxillin: a crossroad in pathological cell migration. J Hematol Oncol. 2017;10:50.
8. Salgia R, Li JL, Lo SH, Brunkhorst B, Kansas GS, Sobhany ES, et al. Molecular cloning of human paxillin, a focal adhesion protein phosphorylated by P210BCR/ABL. J Biol Chem. 1995;270:5039–47.
9. Tumbarello DA, Brown MC, Hetey SE, Turner CE. Regulation of paxillin family members during epithelial-mesenchymal transformation: a putative role for paxillin delta. J Cell Sci. 2005;118:4849–63.
10. Li HG, Xie DR, Shen XM, Li HH, Zeng H, Zeng YJ, et al. Clinicopathological significance of expression of paxillin, syndecan-1 and EMMPRIN in hepatocellular carcinoma. World J Gastroenterol. 2005;11:1445–51.
11. Zhang Z, Peng Z, Cao J, Wang J, Hao Y, Song K, et al. Long noncoding RNA PXN-AS1-L promotes non-small cell lung cancer progression via regulating PXN. Cancer Cell Int. 2019;19:20.
12. Hardivillé S, Banerjee PS, Selen Alpergin ES, Smith DM, Han G, Ma J, et al. TATA-box binding protein O-GlcNAcylation at T114 regulates formation of the B-TFIID complex and is critical for metabolic gene regulation. Mol Cell. 2020;77:1143–52.e1147.
13. Patel AB, Greber BJ, Nogales E. Recent insights into the structure of TFIID, its assembly, and its binding to core promoter. Curr Opin Struct Biol. 2020;61:17–24.
14. Vannini A, Cramer P. Conservation between the RNA polymerase I, II, and III transcription initiation machineries. Molecular cell. 2012;45:439–6.
15. Hasegawa Y, Struhl K. Promoter-specific dynamics of TATA-binding protein association with the human genome. Genome Res. 2019;29:1939–50.
16. Han B, Qu Y, Jin Y, Yu Y, Deng N, Wawrowsky K, et al. FOXC1 activates smoothened-independent Hedgehog signaling in basal-like breast cancer. Cell Rep. 2015;13:1046–58.
17. Myatt SS, Lam EWF. The emerging roles of forkhead box (Fox) proteins in cancer. Nat Rev Cancer. 2007;7:847–59.
18. Grimm D, Bauer J, Wise P, Krüger M, Simonsen U, Wehland M, et al. The role of SOX family members in solid tumours and metastasis. Semin Cancer Biol. 2020;67:122–53.
19. Sakai D, Suzuki T, Osumi N, Wakamatsu Y. Cooperative action of Sox9, Snail2 and PKA signaling in early neural crest development. Development. 2006;133:1323–33.
20. Barrallo-Gimeno A, Nieto MA. The Snail genes as inducers of cell movement and survival: implications in development and cancer. Development. 2005;132:3151–61.
21. Franssen B, Alshebeeb K, Tabrizian P, Marti J, Pierobon ES, Lubezky N, et al. Differences in surgical outcomes between hepatitis B- and hepatitis C-related hepatocellular carcinoma: a retrospective analysis of a single North American center. Ann Surg. 2014;260:650–6; discussion 656-658.
22. Luo MY, Zhou Y, Gu WM, Wang C, Shen NX, Dong JK, et al. Metabolic and nonmetabolic functions of PSAT1 coordinate signaling cascades to confer EGFR inhibitor resistance and drive progression in lung adenocarcinoma. Cancer Res. 2022;82:3516–31.
23. Sharp PA. TATA-binding protein is a classless factor. Cell. 1992;68:819–21.
24. Yuan J, Liu X, Wang T, Pan W, Tao Q, Zhou W, et al. The MBNL3 splicing factor promotes hepatocellular carcinoma by increasing PXN expression through the alternative splicing of lncRNA-PXN-AS1. Nat Cell Biol. 2017;19:820–32.
25. Wen L, Zhang X, Zhang J, Chen S, Ma Y, Hu J, et al. Paxillin knockdown suppresses metastasis and epithelial-mesenchymal transition in colorectal cancer via the ERK signalling pathway. Oncol Rep. 2020;44:1105–5.
26. Yang JD, Hainaut P, Gores GJ, Amadou A, Plymoth A, Roberts LR. A global view of hepatocellular carcinoma: trends, risk, prevention and management. Nat Rev Gastroenterol Hepatol. 2019;16:589–604.
27. Rowlands T, Baumann P, Jackson SP. The TATA-binding protein: a general transcription factor in eukaryotes and archaebacteria. Science. 1994;264:1326–9.
28. He Y, Fang J, Taatjes DJ, Nogales E. Structural visualization of key steps in human transcription initiation. Nature. 2013;495:481–6.
29. Di Pietro C, Ragusa M, Duro L, Guglielmino MR, Barbagallo D, Carnemolla A, et al. Genomics, evolution, and expression of TBPL2, a member of the TBP family. DNA Cell Biol. 2007;26:369–85.

30. Kawakami E, Adachi N, Senda T, Horikoshi M. Leading role of TBP in the establishment of complexity in eukaryotic transcription initiation systems. Cell Rep. 2017;21:3941–56.

31. Pascual M, Vicente M, Monferrer L, Artero R. The Muscleblind family of proteins: an emerging class of regulators of developmentally programmed alternative splicing. Differentiation. 2006;74:65–80.

32. Yu Z, Wang G, Zhang C, Liu Y, Chen W, Wang H, et al. LncRNA SBF2-AS1 affects the radiosensitivity of non-small cell lung cancer via modulating microRNA-302a/MBNL3 axis. Cell Cycle. 2020;19:300–16.

33. Sun X, Diao X, Zhu X, Yin X, Cheng G. Nanog-mediated stem cell properties are critical for MBNL3-associated paclitaxel resistance of ovarian cancer. J Biochem. 2021;169:747–56.

34. Zhou HZ, Li F, Cheng ST, Xu Y, Deng HJ, Gu DY, et al. DDX17-regulated alternative splicing that produced an oncogenic isoform of PXN-AS1 to promote HCC metastasis. Hepatology. 2022;75:847–65.

35. Xiao R, Chen JY, Liang Z, Luo D, Chen G, Lu ZJ, et al. Pervasive chromatin-RNA binding protein interactions enable RNA-based regulation of transcription. Cell. 2019;178:107–21. e118.

36. Han H, Braunschweig U, Gonatopoulos-Pournatzis T, Weatheritt RJ, Hirsch CL, Ha KCH, et al. Multilayered control of alternative splicing regulatory networks by transcription factors. Mol Cell. 2017;65:539–3 e537.